Geotech Geol Eng (2016) 34:1737–1748
DOI 10.1007/s10706-016-9985-x

ORIGINAL PAPER

Effect of Gas Pressure on Rock Burst Proneness Indexes and Energy Dissipation of Coal Samples

Yi Xue · Feng Gao · Teng Teng · Yan Xing

Received: 17 October 2015 / Accepted: 20 January 2016 / Published online: 25 January 2016
© Springer International Publishing Switzerland 2016

Abstract To investigate the influence of gas pressure on rock burst proneness of coal, the rock burst proneness tests were conducted under different gas pressures. Based on the energy method, the rock burst proneness and energy accumulation law are analyzed. The following conclusions can be drawn: (1) The change laws of impact energy index, the effective impact energy index and the residual energy index are consistent, reducing with the increase of gas pressure. (2) Before the coal failure, the total energy, the elastic energy, and the dissipated energy of coal specimens increase with the increase of the stress. The increase speed of total energy is the fastest, the elastic energy takes the second place, and the dissipated energy is the slowest. (3) The failure energy ratio and stress drop coefficient defined by energy can be used to describe the rock burst proneness. (4) The failure modes of coal samples transform from brittle failure into ductile shear failure with the increase of gas pressure. (5) In the coal seam which has typical dynamic hazards, there is a critical value of gas pressure. When the gas pressure is higher than the critical value, gas outburst is the main disaster. When the gas pressure is lower than the critical value, the rock burst is the main disaster.

Keywords Gas pressure · Rock burst · Energy dissipation · Failure mode

1 Introduction

Rock burst is a kind of coal mine dynamic disaster and seriously threatens the safety of coal mine. With the increase in coal mining depth, the occurrence frequency and intensity of rock burst are increasing (Kabiesz 2006; Jiránková 2010). Besides, rock burst can trigger many other mine disasters, e.g. gas explosion, coal dust explosion, fire hazard and underground water inrush. And even the serious rock burst can cause the ground shaking and building damage (He et al. 2010; Bukowska 2013; Song et al. 2014; Mazaira and Konicek 2015). Therefore, rock burst is one of the major disasters in coal mine.

In recent years, scholars have carried out lots of fruitful research on rock burst in coal mines. Li et al. (2005) found that both rock burst and earthquakes could trigger unusual gas emission through a great deal of microseismic monitoring, gas monitoring and field investigation, and suggested that the relationship between rock burst hazard and gas disaster should be

Y. Xue (✉) · F. Gao · T. Teng
State Key Laboratory for Geomechanics and Deep Underground Engineering, China University of Mining and Technology, Xuzhou 221116, China
e-mail: xueyixy@126.com

Y. Xing
Rock Mass Modeling and Computational Rock Mechanics Laboratories, University of Arizona, Tucson, AZ 85721, USA

paid more attention in the deep coal mining. He et al. (2010) evaluated the rock burst hazards in deep coal mine with the active velocity tomography and verified the accuracy and efficiency of the tomography through micro-seismic events. Chen et al. (2012) analyzed the variation features of microseismic energy releasing and microseismic frequency and suggested that the weak seismic activity showed energy accumulation for strong shock, which could be used to forecast the danger of rock burst. Yan et al. (2015) suggested the development of rock bursts depends on the in situ stress and the brittleness of rocks. Decreasing the stress of surrounding rocks and the disturbance from the excavation are the main methods for controlled blasting.

However, the study about the quantitative evaluation of the influence of gas pressure on rock burst is less. In the deep coal exploitation, the coal seam is not only influenced by the high in situ stress, but also influenced by high gas pressure. After the excavation, the surrounding rocks are usually damaged due to the effect of in situ stress, the power of the external force is transformed into the dissipated energy, and the elastic energy accumulated in coal releases gradually. If the gas can release from the coal seam, it will not provide the additional energy to the rock burst. However, if the permeability of coal seam is low and gas cannot release easily, gas will be involved in the process of the occurrence of rock burst, and gas expansion can develop the impact of rock burst (Wang et al. 2010; Mutke et al. 2015). It can be seen that in the process of mining the coal seams with rock burst proneness, there exists a coupled effect of rock burst and gas outburst. Therefore, it is necessary to carry out the research on the influence of gas on the coal seams with rock burst proneness.

To investigate the influence of gas pressure on rock burst proneness of coal, the rock burst proneness tests were conducted under different gas pressures. Based on the energy method, the rock burst proneness and energy accumulation laws were analyzed and the failure modes of the coal samples were analyzed with the acoustic emission (AE) location technology.

2 Experimental Procedures

The mechanical tests of the gas-saturated coal are usually measured under triaxial compression, that is, the oil pressure is loaded around the coal samples to seal the gas in the coal samples. According to the *classification and laboratory test method on bursting liability of coal* (Professional Standards Compilation Group of People's Republic of China 2010), the rock burst index is measured with the standard raw coal sample under uniaxial compression with a certain loading rate. However, the sealing method should be considering because of the existence of gas. In the tests, the MTS815 mechanical testing system was used to maintain a certain confining pressure, gas was sealed in coal samples by shrink film. Then the axial pressure was loaded gradually. Although there is a difference between the triaxial compression test and uniaxial compression test, the change laws are similar and the influence of gas pressure on rock burst proneness indexes of the coal samples can be studied (Song et al. 2015).

The coal samples were taken from the Pingdingshan mine, Henan province, China. The thickness of the coal seam is basically stable, about 3.2–3.9 m; the dip angle of the coal seam was 17°–25°. The gas pressure of the coal seam was 1.5–2.0 MPa and the gas content was 20–22 m^3/t, belonging to the high gas and low permeability coal seam. The standard coal samples were prepared, with diameter 50 mm and height 100 mm.

The MTS815 Flex Test GT mechanical test system was used (Fig. 1). The methane volume ratio was 99.99 %, the gas pressure was 1, 2, 3 and 5 MPa, and the confining pressure was 10 MPa. Firstly, using the force control mode, the 3 MPa/min was applied to reach the hydrostatic pressure 10 MPa. Then the confining pressure was kept constant, the methane entered the pressure cylinder and the gas pressure reached the set gas pressure (1, 2, 3 and 5 MPa). Until the coal samples reached the adsorption saturation, the force control mode was used with axial loading speed of 10 MPa/min. In order to protect the test equipment, the displacement control mode was used with the speed of 0.04 mm/min when the coal was in the post-peak stage.

PCI-2 acoustic emission (AE) system was used to record the cracking process. In the test, eight sensors were attached to specimen to obtain the spatial distribution of acoustic emission (AE) events, and the sampling rate was 40 m/s. The used AE sensors were Mic30 sensors with a central frequency of 300 kHz, and a frequency range from 150 to

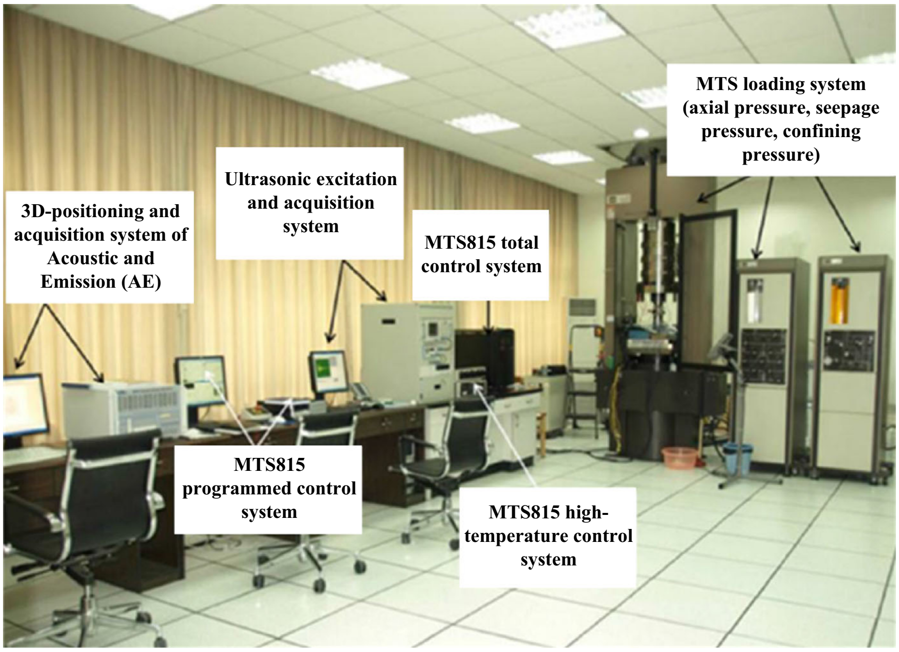

Fig. 1 MTS815 Flex Test GT

1000 kHz. The preamplifier gain was 40 dB, and the threshold was fixed at 30 dB. In the tests, 8 acoustic emission sensors (1#–8#) were fixed on the surface of the specimen, and 4 AE sensors were placed on the both ends of the specimen respectively, as shown in Fig. 2. Using the Geiger locating algorithm which was based on least square method, the AE location function was achieved and the spatial location of acoustic emission source was got according to the time difference of P wave received by sensors in different positions.

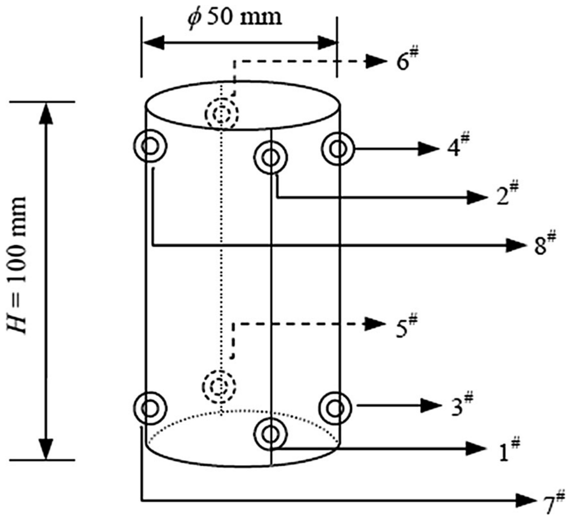

Fig. 2 Sketch of acoustic emission (AE) sensors arrangement

3 Effect of Gas Pressure on Rock Burst Proneness Indexes of Coal Samples

3.1 Rock Burst Proneness Indexes

The rock burst proneness of rock can be measured by the rock burst proneness tests. Scholars have put forward many effective rock burst proneness indexes which are widely used, such as elastic energy index, impact energy index, dynamic failure time, effective impact energy index, residual energy index, energy storage index, elastic deformation index, stiffness ratio index, brittleness coefficient, etc.

The elastic energy index W_{ET} is defined as the ratio of the elastic strain energy and the strain energy dissipation at point E (75–85 % of the peak strength). As shown in Fig. 3, the ratio of the area S_{EAC} (between the unloaded line EA and the strain axis) and the area S_{EOA} (between the load and unload line) is the elastic energy index, i.e. $W_{\mathrm{ET}} = S_{EAC}/S_{EOA}$. Generally, strong rock burst proneness, $W_{\mathrm{ET}} \geq 5.0$; medium rock

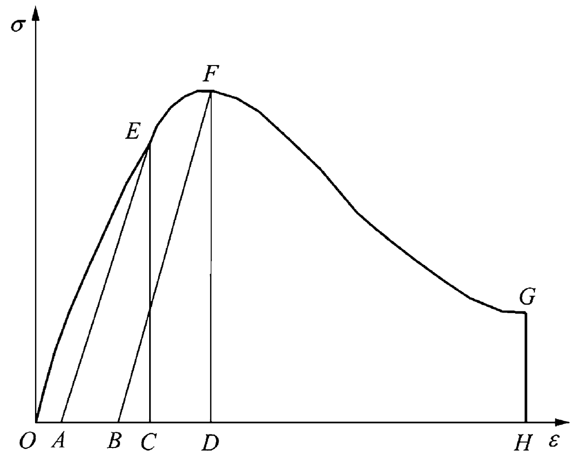

Fig. 3 Complete stress–strain curve of coal samples

burst proneness, $2.0 \leq W_{ET} < 5.0$; no rock burst proneness, $W_{ET} < 2.0$.

The impact energy index K_E is defined as the ratio of the pre-peak area and the post-peak area, $K_E = S_{OEFD}/S_{FDHG}$, namely, the ratio of energy in the pre-peak stage and the energy released in the post-peak stage. Generally, strong rock burst proneness, $K_E > 2.0$; medium rock burst proneness, $1.0 \leq K_E < 2.0$; no rock burst proneness, $K_E < 1.0$.

The effective impact energy index K_{eff} combines the elastic energy index W_{ET} and impact energy index W_E, defined as the ratio of the elastic energy in the pre-peak stage and the dissipated energy in the post-peak stage. That is, the ratio of the area S_{FBD} under the unloading curve FB and the area S_{FDHG} in the in the post-peak stage, $K_{eff} = S_{FBD}/S_{FDHG}$.

The residual energy index W_R is the ratio of the surplus energy and the dissipated energy in the post-peak stage, $W_R = (S_{FBD} - S_{FDHG})/S_{FDHG}$.

The stiffness ratio is defined as the ratio of the stiffness before the yield point K_f and the stiffness after the yield point $|K_b|$, $K_{fb} = K_f/|K_b|$.

3.2 Change Law of Rock Burst Proneness Indexes

Based on the definition of the above indexes, the energy can be obtained by the integral of the stress–strain curve at the different stages, and then the indexes values can be obtained through the calculation. It is assumed the gradient of unloading line in the elastic stage is the same as that of the loading line in the elastic stage (Zhang et al. 2010; Xu et al. 2011; Konicek et al. 2013; Xia et al. 2014; Song et al. 2015), and then the elastic energy can be calculated. The calculated values of the 5 indexes under different gas pressures are shown in Table 1.

Figure 4 shows the changes of the burst proneness indexes under different gas pressure. The fitting curves of data points of two coal samples at different gas pressures are also showed in Fig. 4. The impact energy index, the effective impact energy index and the residual energy index correspond the left vertical coordinate while the elastic energy index corresponds the right vertical coordinate. It can be seen from Table 1 and Fig. 4 that with the increase of gas pressure, the impact energy index, the effective impact energy index and the residual energy index decrease gradually. This decrease is not so obvious when gas pressure is between 2 and 3 MPa. The change of rock burst proneness indexes along with the gas pressure is presented as follows:

1. When the gas pressure is 1 MPa, rock burst proneness indexes of coal samples are comparatively high. It has a strong burst tendency according to the elastic energy index. The rock burst proneness is moderately strong according to the impact energy index. This shows that the coal sample is brittle and it is easy to release a large amount of strain energy during the loading process.
2. The change laws of impact energy index, the effective impact energy index and the residual energy index are consistent, reducing with the increase of the gas pressure. When the gas pressure increases from 1 to 2 MPa, the rock burst proneness indexes of rock drops significantly, the impact energy index decreases by 43 %. When the gas pressure increases from 2 to 5 MPa, these three rock burst proneness indexes continue to fall, reaching to the lowest value.
3. With the increase of gas pressure, the stiffness ratio is increasing although fluctuation exists. The rock burst proneness changes from medium tendency to low tendency. Therefore, the change law of the stiffness ratio is consistent with elastic energy index.

3.3 Correlations of Impact Indexes

The rock burst tendency is the property which reflects the compressive strength, the storage energy, the

Table 1 Energy indices and rigidity ratios of rock samples at different gas pressure

Number	Gas pressure (MPa)	Elastic energy index	Impact energy index	Effective impact energy index	Residual energy index	Stiffness ratio
T1	1	9.97	1.53	1.29	0.29	0.38
T2	1	26.29	3.59	3.23	2.23	0.16
T3	2	10.22	0.62	0.53	−0.47	0.23
T4	2	20.19	1.61	1.37	0.37	0.12
T5	3	3.21	1.86	1.21	0.21	0.41
T6	3	3.80	1.50	1.12	0.12	0.47
T7	5	4.54	1.01	0.73	−0.27	0.77
T8	5	28.73	0.51	0.44	−0.56	8.37

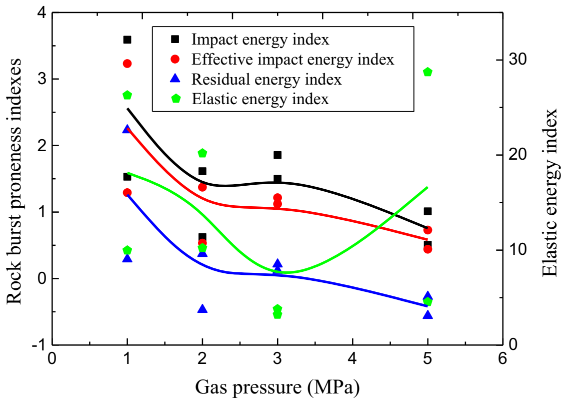

Fig. 4 Changes in rock burst proneness indexes with gas pressure

energy dissipation, and the failure speed of coal samples. Although different indexes are comparatively independent, there is a correlation between each index. All of these indexes reflect the impact tendency from different mechanisms. Compressive strength reflects the bearing capacity of coal samples. Elastic energy index, impact energy index and residual energy index are the relative energy relationships. They reflect the energy ratio and are not influenced by the concrete value of energy. For the same coal seam, the values of rock burst tendency indexes are discrete due to the heterogeneity of coal samples, but there still is a certain correlation between the indexes. More measurements were conducted to investigate the correlations of impact indexes of coal samples.

Figure 5 shows the correlations between the effective impact energy index, elastic energy index, impact energy index, residual energy index and compressive strength. It can be seen from Fig. 5 that although the coal samples are discrete, it has a good correlation between these indexes, which explains the rationality of these indexes. It can be seen from Fig. 5a that the elastic energy index grows with the increase of the effective impact energy index. It can be seen from Fig. 5b that although there is a poor correlation between the residual energy index and elastic energy index, the higher residual energy index usually means the higher elastic energy index. It can be seen from Fig. 5c that the correlation between impact energy index and effective impact energy index is good and the impact energy index is higher when effective impact energy index is higher. It can be seen from Fig. 5d that a good correlation between impact energy index and residual energy index exists, that is, when the impact energy index is higher, the energy released in the post-peak stage is bigger and the rock burst risk is higher. It can be seen from Fig. 5e that the higher the compressive strength of coal sample corresponds the higher impact energy index. When the compressive strength is higher, the coal can store up more energy released when it is broken. This phenomenon is consistent with the research results obtained by Su et al. (2013). It can be seen from Fig. 5f that the coal sample with higher compressive strength has the ability to bear bigger deformation and store up more deformation energy in the loading process, so the rock burst proneness is higher. To sum up, there is a positive correlation between effective impact energy index, elastic energy index, impact energy index, residual energy index and compressive strength of coal samples. That is, these indexes can reflect the rock burst proneness effectively.

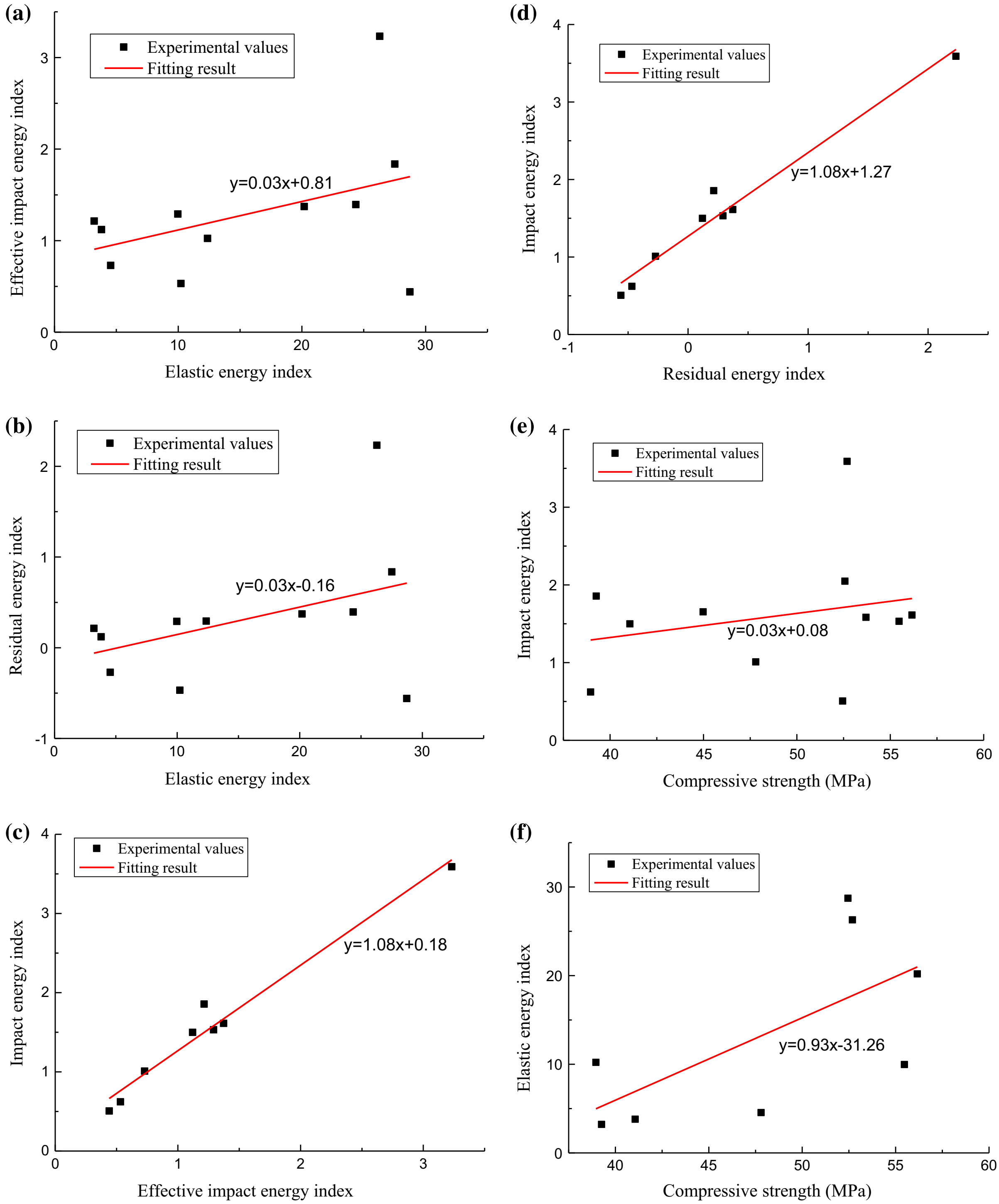

Fig. 5 The correlations between effective impact energy index, elastic energy index, impact energy index, residual energy index and compressive strength. **a** The relationship between effective impact energy index and elastic energy index, **b** the relationship between residual energy index and elastic energy index, **c** the relationship between impact energy index and effective impact energy index, **d** the relationship between impact energy index and residual energy index, **e** the relationship between impact energy index and compressive strength, **f** the relationship between elastic energy index and compressive strength

4 Energy Dissipation Law of Coal Under Different Gas Pressures

4.1 Energy Dissipation Law of Coal

Energy dissipation is the essential property of rock failure, and energy method is a common method used to analyze the failure process of rock. The failure process of material is the process of energy accumulation and energy dissipation and the process of energy evolution in the interior of material. During the loading process, rock deformation emerges due to the effect of external force. The elastic energy U_e under conventional triaxial compression is given by the following (Xie et al. 2009).

$$U_e = \frac{1}{2}\sigma_1\varepsilon_1^e + \frac{1}{2}\sigma_2\varepsilon_2^e + \frac{1}{2}\sigma_3\varepsilon_3^e = \frac{1}{2E_0}\left[\sigma_a^2 + 2(1-v_0)\sigma_{cf}^2 - 4v_0\sigma_a\sigma_{cf}\right] \quad (1)$$

The work done by the vertical load can be calculated as follows (Xie et al. 2009).

$$W = \int \sigma_a \varepsilon_a \mathrm{d}\varepsilon_a \quad (2)$$

During the loading process, following equation can be obtained based on the first law of thermodynamics:

$$W = U_d + U_e \quad (3)$$

where U_d is the energy dissipated by the rock in the process of loading, which is used for the damage and the plastic deformation of rock; U^e is the elastic strain energy stored in rock.

Therefore, the energy dissipated up to the peak strength is the difference between the work done and the elastic energy (Peng et al. 2015)

$$U_{d1} = W_c - U_{ec} = \int_0^{\varepsilon_{tc}} \sigma_a\varepsilon_a \mathrm{d}\varepsilon_a - \frac{\sigma_a^2 + 2(1-v_0)\sigma_{cf}^2 - 4v_0\sigma_a\sigma_{cf}}{2E_0} \quad (4)$$

where W_c is the total work done by the vertical load before the peak strength; U_{ec} is the elastic energy at the peak strength; ε_{tc} is the vertical strain at the peak strength.

The energy released during the stress drop is calculated by

$$U_r = U_{ec} - U_{ed} \quad (5)$$

where U_{ed} is the elastic energy at the drop stress. Both U_{ec} and U_{ed} can be calculated using Eq. (1) by substituting σ_{tc} and σ_d for σ_a, respectively.

Further, the energy dissipated during the stress drop process can be calculated as (Peng et al. 2015).

$$U_{d2} = \int_{\varepsilon_{tc}}^{\varepsilon_d} \sigma_a\varepsilon_a \mathrm{d}\varepsilon_a \quad (6)$$

The relationship between elastic energy and dissipated energy is shown in Fig. 6.

Rock burst is the process of energy conversion in various forms. Therefore the energy change laws of coal samples are studied to investigate the effect of gas pressure on rock burst. The total energy W, elastic energy U_e and dissipated energy U_d are calculated by Eqs. (1)–(3).

According to the experiments and the energy computational formulae, the energy consumption characteristics of the coal samples under different gas pressures can be obtained, as shown in Fig. 7. In the initial compression phase, the change of dissipated energy is very small, and there is almost no growth in the elastic stage. The majority of total work done by the external force is transformed into elastic energy of coal samples. When the coal samples are close to the peak strength, i.e., the failure point, coal samples begin to generate new micro cracks in the interior of the coal samples, resulting in the slight increase in dissipated energy. When the coal samples reach the failure point, the elastic energy of coal sample reaches the maximum, then coal samples is in the state of limit equilibrium. Any weak energy disturbance will lead to sudden release of elastic energy and result in the

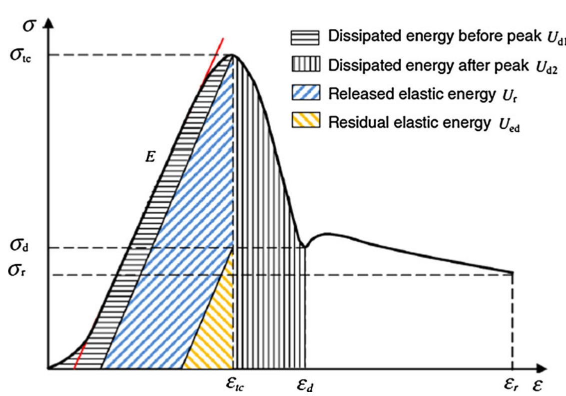

Fig. 6 Calculation of dissipated energy and released energy (Peng et al. 2015)

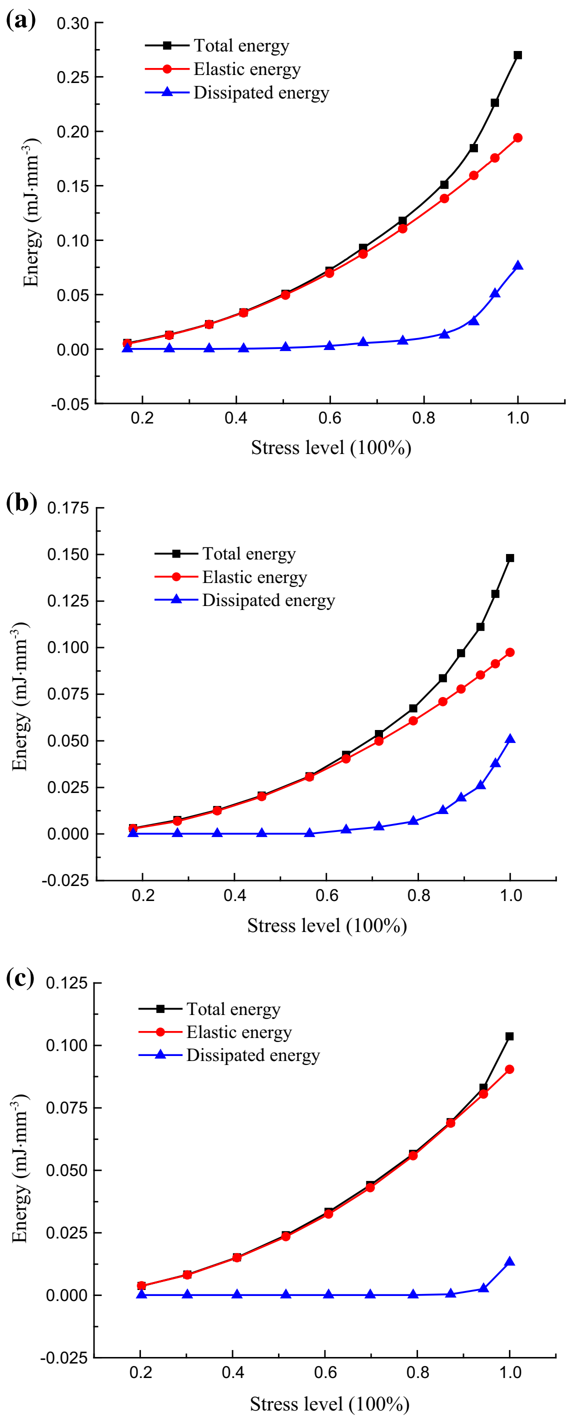

Fig. 7 Evolution curves of energy under different gas pressure. **a** Gas pressure 1 MPa, **b** gas pressure 2 MPa, **c** gas pressure 3 MPa

failure of coal. When the coal sample is broken, the energy liberates in large quantity. The energy is transformed to the fracture surface energy of coal sample and the kinetic energy, acoustic, electromagnetic wave energy, etc. (Song et al. 2015).

Before the failure, the total energy, the elastic energy, and the dissipated energy of the specimens increase with the increase of the stress. The increase speed of total energy is the fastest, the elastic energy takes the second place, and the dissipated energy is the slowest. With the increase in gas pressure, the increases in total energy, elastic energy and dissipated energy show a decreasing trend. When the gas pressure is high, the elastic energy of coal samples becomes small. The energy released during the failure process becomes small, which reduces the rock burst tendency. Therefore, high gas pressure weakens the rock burst tendency of coal samples.

4.2 Failure Energy Ratio

The failure of coal samples is casued by the energy dissipation and energy release. According Fig. 6, the failure energy is defined as

$$U_f = U_{d1} + U_{d2} + U_r \tag{7}$$

The failure of the coal samples is not affected by the energy dissipation in the residual phase, and the energy dissipation in the residual stage only further induces the development of the damage, so the energy dissipated of the residual phase is neglected.

The failure energy ratio is defined as the ratio between the failure energy and the total work (Peng et al. 2015)

$$\beta = \frac{U_f}{W_d} = 1 - \frac{U_{ed}}{W_d} \tag{8}$$

where W_d is the total work before the residual stage.

Figure 8 shows the failure energy ratio of coal samples under different gas pressures. When the total work done by the external load is constant, the higher residual elastic energy means the smaller failure energy and smaller energy released during the failure. Therefore, when failure energy ratio is 0, it is an ideal reversible elastic process without failure. When failure energy ratio is 1, it is an ideal brittle failure process without any residual stress. The value of failure energy ratio is related to the failure mode of rock samples. Therefore, the failure energy ratio can be used to describe the rock burst proneness. When failure energy ratio is smaller, the smaller energy releases during the failure and the rock burst proneness is lower.

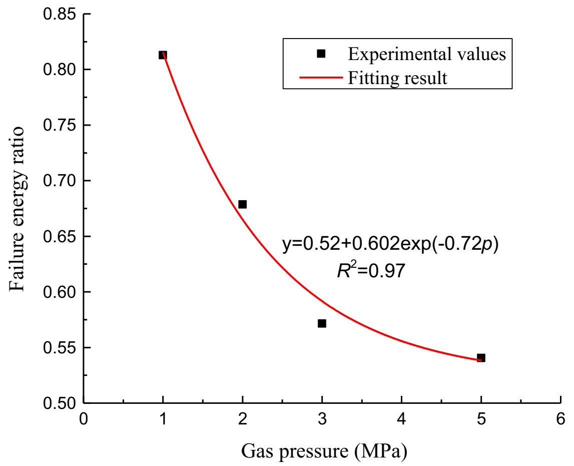

Fig. 8 Failure energy ratio of coal samples under different gas pressures

4.3 Stress Drop Coefficient

The failure mechanism of coal samples changes with the change of gas pressure. Figure 9 shows that the failure modes of coal samples changes from the brittle failure to ductile failure with the increase of gas pressure. It means that the failure mechanism of coal samples under low gas pressure is different from that of high gas pressure. The stress drop coefficient reflects the softening extent and the brittleness of the rock material. Based on the stress strain characteristics, the stress drop coefficient is usually used to describe the brittle characteristics of rock (Zheng et al. 2005).

$$R = \frac{\varepsilon_d - \varepsilon_{tc}}{\varepsilon_{tc} - \sigma_d / E} \tag{9}$$

However this definition neglects the effect of stress drop $\sigma_{tc} - \sigma_d$. Based on the energy dissipation and energy release, the ratio between the elastic energy and the dissipated energy is defined as the drop coefficient stress (Peng et al. 2015).

$$\alpha = \frac{U_r}{U_{d1} + U_{d2}} \tag{10}$$

When stress drop coefficient $\alpha = \infty$, it means the ideal brittle failure without energy dissipation, as shown in Fig. 9a. When stress drop coefficient $\alpha = 0$, it means the ideal ductile failure without energy release, as shown in Fig. 9b. When stress drop coefficient α is between 0 and ∞, it means the normal failure mode and both of energy release and energy dissipation exist during this failure process, as shown in Fig. 9c. When the gas pressure increases, the failure mode of coal samples changes from the brittle failure to ductile failure, the stress–strain curves changes from Fig. 9a, b, finally approaching Fig. 9c. Figure 10 shows the stress drop coefficient of coal failure under different gas pressures. It can be seen that stress drop coefficient of coal samples decreases with the increase of gas pressure. Therefore, the stress drop coefficient can be used to describe the rock burst proneness.

The rock burst tendencies of these three stress–strain curves decrease in turn. A large amount of elastic strain is accumulated in the coal sample which has the stress–strain curve as Fig. 9a. The energy dissipation caused by plastic deformation is relatively small. Therefore, when the external stress exceeds the peak strength, a large number of elastic strain energy accumulated in coal samples releases suddenly and violently. The impact energy index is large and the coal sample has a strong rock burst tendency. The structure changes gradually with the increase of load for the coal sample which has the stress–strain curve as Fig. 9b. The coal sample remains intact after its failure and accumulates large elastic strain energy, belonging to the medium rock burst tendency. The majority of the elastic energy changes to the plastic energy in the coal sample which is similar to Fig. 9c. The macroscopic cracks are produced gradually. The elastic energy is exhausted during the failure process,

Fig. 9 Demonstration of stress drop coefficient of failure. **a** Ideal brittle failure, **b** common failure, **c** ideal ductile failure

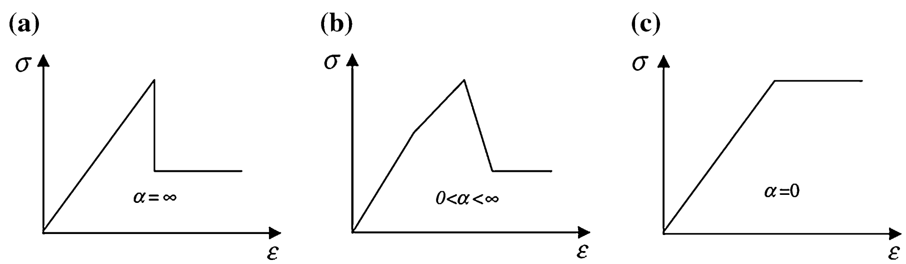

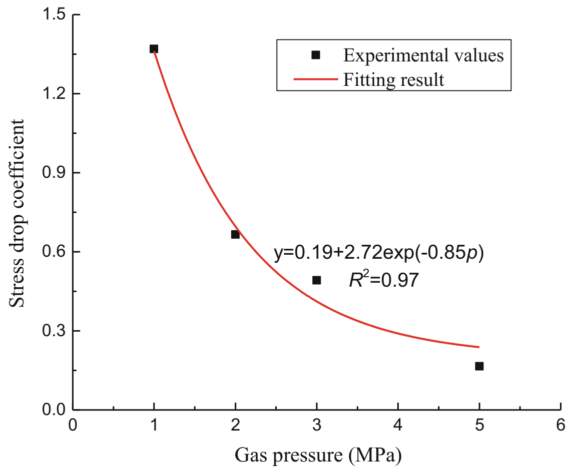

Fig. 10 Stress drop coefficient of coal failure under different gas pressures

converting to the plastic potential energy, showing no rock burst tendency.

4.4 Analysis of Failure Mode

Table 2 shows the spatial distributions of acoustic emission (AE) events in different stress levels during the loading process. Using the 3D acoustic emission (AE) location technology, the fracture evolution characteristics of the coal samples can be understood. With the increase of gas pressure, the stress drop degree of coal samples decreases gradually, and the coal samples change gradually from brittle failure to ductile failure. The surface cracks are mainly some axial splitting cracks under low gas pressure. The surface cracks gradually become some inclined shear cracks or X-form shear cracks under high gas pressure. The failure modes of coal samples transform from brittle failure into ductile shear failure. It is possibly because the gas adsorption weakens the bond strength between coal particles and causes a certain degree of softening of coal samples. It also weakens the brittle failure of coal samples. At the same time, it can be seen that the stress level where the initial release point of AE energy emerges becomes lower and lower with the increase of gas pressure. The more energy releases at the lower stress level with the higher gas pressure, and more energy dissipation occurs during the loading process, so the energy released at the failure point becomes smaller and the rock burst tendency becomes lower.

5 Discussion on Coupled Hazards of Gas Burst and Rock Burst

The above results show that the gas pressure has a great influence on the rock burst tendency of coal. However the current study about rock burst does not consider the influence of gas. The coal seams contain lots of adsorbed gas and free gas. 90 % of the gas is adsorbed in the pores and cracks of coal mass (Connell 2009; Xue et al. 2014; Xia et al. 2015). Adsorbed gas changes the mechanical properties of coal mass and reduces the peak strength of coal mass, so that the coal is more vulnerable to damage under the effect of in situ stress. Therefore, the coupled hazards of gas outburst and rock burst may happen under the coupled effect of high stress and high gas pressure in deep coal mine.

Based on the above analysis, it can be drawn that the existence of gas reduces the rock burst tendency of coal seam. The coal seam has low rock burst tendency when the gas pressure is high. However, the probability of occurrence of gas outburst increases significantly especially in the high in situ stress area. Therefore, in the coal seam with typical dynamic hazards, there is a critical value of gas pressure. When the gas pressure is higher than the critical value, gas outburst is the main disaster. When the gas pressure is lower than the critical value, the rock burst is the main disaster.

6 Conclusion

To investigate the influence of gas pressure on rock burst proneness of coal, the rock burst proneness tests were conducted under different gas pressures. Based on the energy method, the rock burst proneness and energy accumulation laws were analyzed and the failure modes of the coal samples were analyzed with the acoustic emission (AE) location technology. The following conclusions can be drawn:

1. The change laws of impact energy index, the effective impact energy index and the residual energy index are consistent, reducing with the increase of gas pressure. There is a positive correlation between effective impact energy index, elastic energy index, impact energy index, residual energy index and compressive strength of coal samples.

Table 2 Spatial distribution of acoustic emission (AE) events at different stress levels for coal samples under different gas pressures

Gas pressure	Stress level 20 %	60 %	80 %	90 %	100 %	Post-peak 80 %	Failure mode
1 MPa	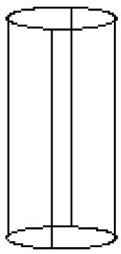	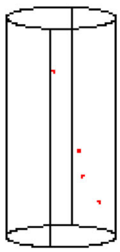	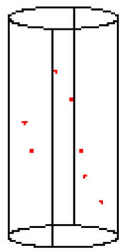	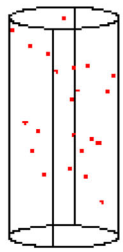	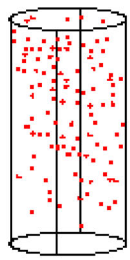	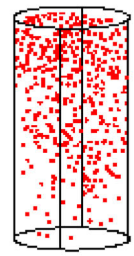	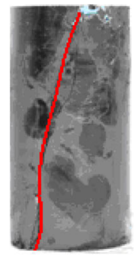
2 MPa	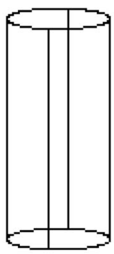	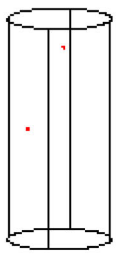	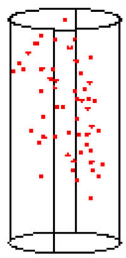	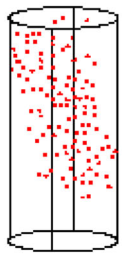	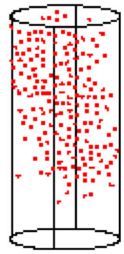	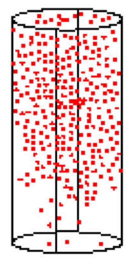	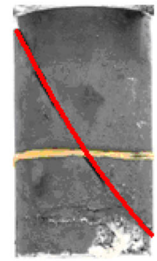
3 MPa	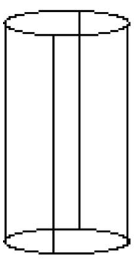	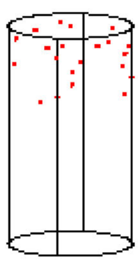	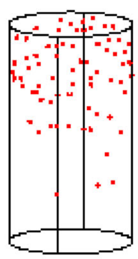	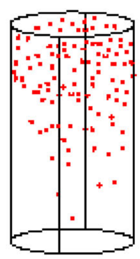		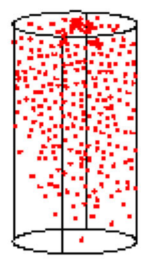	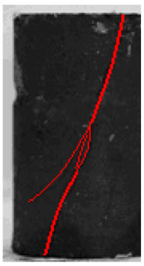
5 MPa	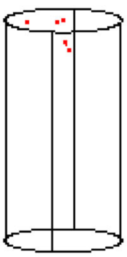	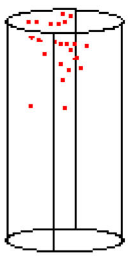	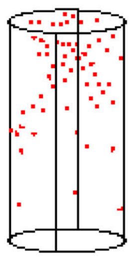	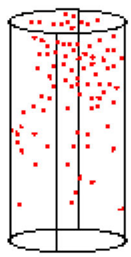	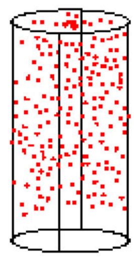	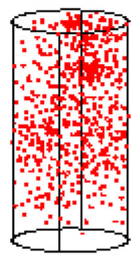	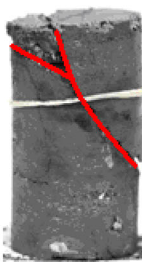

2. Before the failure, the total energy, the elastic energy, and the dissipated energy of the specimens increase with the increase of the stress. The increase speed of total energy is the fastest, the elastic energy takes the second place, and the dissipated energy is the slowest. High gas pressure weakens the rock burst tendency of coal samples.
3. The failure energy ratio and stress drop coefficient defined by energy can be used to describe the rock burst proneness. When failure energy ratio and

stress drop coefficient are smaller, the plastic characteristic is more obvious, the smaller energy releases during the failure and the rock burst proneness is lower.

4. The surface cracks are mainly some axial splitting cracks under low gas pressure. The surface cracks gradually become some inclined shear cracks or X-form shear cracks under high gas pressure. The failure modes of coal samples transform from brittle failure into ductile shear failure with the increase of gas pressure.
5. The coal seam has low rock burst tendency when the gas pressure is high. In the coal seam with typical dynamic hazards, there is a critical value of gas pressure. When the gas pressure is higher than the critical value, gas outburst is the main disaster. When the gas pressure is lower than the critical value, the rock burst is the main disaster.

Acknowledgments The authors are grateful to the financial support from the National Natural Science Foundation of China (51404250), the Natural Science Foundation of Jiangsu, China (BK20140189), the China Postdoctoral Science Foundation (2014M550315) and the College Graduate Research and Innovation Program of Jiangsu Province (KYLX15_1408).

References

Bukowska M (2013) Post-peak failure modulus in problems of mining geo-mechanics. J Min Sci 49(5):731–740

Chen XH, Li WQ, Yan XY (2012) Analysis on rock burst danger when fully-mechanized caving coal face passed fault with deep mining. Saf Sci 50(4):645–648

Connell LD (2009) Coupled flow and geomechanical processes during gas production from coal seams. Int J Coal Geol 79(1):18–28

He MC, Miao JL, Feng JL (2010) Rock burst process of limestone and its acoustic emission characteristics under true-triaxial unloading conditions. Int J Rock Mech Min Sci 47(2):286–298

Jiránková E (2010) Assessment of rigid overlying strata failure in face mining. Central Eur J Geosci 2(4):524–530

Kabiesz J (2006) Effect of the form of data on the quality of mine tremors hazard forecasting using neural networks. Geotech Geol Eng 24(5):1131–1147

Konicek P, Soucek K, Stas L, Singh R (2013) Long-hole destress blasting for rockburst control during deep underground coal mining. Int J Rock Mech Min Sci 61:141–153

Li T, Cai MF, Wang JA, Li DC, Liu J (2005) Discussion on relativity between rockburst and gas in deep exploitation. J China Coal Soc 30(5):562–567

Mazaira A, Konicek P (2015) Intense rockburst impacts in deep underground constructions and their prevention. Can Geotech J 52(10):1426–1439

Mutke G, Dubiński J, Lurka A (2015) New criteria to assess seismic and rock burst hazard in coal mines. Arch Min Sci 60(3):743–760

Peng R, Ju Y, Wang JG, Xie H, Gao F, Mao L (2015) Energy dissipation and release during coal failure under conventional triaxial compression. Rock Mech Rock Eng 48(2):509–526

Professional Standards Compilation Group of People's Republic of China. Classification and laboratory test method on bursting liability of coal (GT/T25217.2–2010). Beijing, Standards Press of China, 2010

Song DZ, Wang EY, Liu ZT, Liu XF, Shen RX (2014) Numerical simulation of rock–burst relief and prevention by water–jet cutting. Int J Rock Mech Min Sci 70:318–331

Song ZL, Han PB, Li WP, Yin GZ, Li MH, Kang XT (2015) Impact of energy dissipation of coal samples with rockburst tendency from gas in its failure process. J China Coal Soc 40(4):843–849

Su CD, Yuan RF, Zhai XX (2013) Experimental research on bursting liability index of coal samples of Chengjiao mine. Chin J Rock Mech Eng 32(S2):3696–3704

Wang Z, Yin GZ, Hu QT, Jin HW (2010) Inducing and transforming conditions from rockburst to coal–gas outburst in a high gassy coal seam. J Min Safety Eng 27(4):572–575

Xia TQ, Zhou FB, Liu J, Kang JH, Gao F (2014) A fully coupled hydro-thermo-mechanical model for the spontaneous combustion of underground coal seams. Fuel 125:106–115

Xia T, Wang X, Zhou F, Kang J, Liu J, Gao F (2015) Evolution of coal self-heating processes in longwall gob areas. Int J Heat Mass Transf 86:861–868

Xie HP, Li L, Peng R, Ju Y (2009) Energy analysis and criteria for structural failure of rocks. J Rock Mech Geotech Eng 1(1):11–20

Xu GA, Niu SJ, Jing HW, Yang SQ, Wang WL (2011) Experimental study of energy features of sandstone under loading and unloading. Rock Soil Mech 32(12):3611–3617

Xue S, Yuan L, Xie J, Wang Y (2014) Advances in gas content based on outburst control technology in Huainan, China. Int J Min Sci Technol 24(3):385–389

Yan P, Zhao ZG, Lu WB, Fan Y, Chen XR, Shan ZG (2015) Mitigation of rock burst events by blasting techniques during deep-tunnel excavation. Eng Geol 188:126–136

Zhang ZZ, Gao F, Liu ZJ (2010) Research on rockbursts proneness and its microcosmic mechanism of granite considering temperature effect. Chin J Rock Mech Eng 29(8):1591–1602

Zheng H, Liu DF, Lee CF, Ge XR (2005) Principle of analysis of brittle–plastic rock mass. Int J Solids Struct 42(1):139–158